Modeling of Heat Generation in Ammonia-Treated Solid Rocket Propellant

Richard L. Raun and K. Bruce Isom
Hercules, Inc., Bacchus Works, Magna, UT 84044

One approach to demilitarize solid rocket propellants is treatment with ammonia. Ammonia extracts the oxidizers ammonium perchlorate and HMX, yielding a solid residue that is more suitable for incineration and less sensitive to impact and other modes of accidental initiation. Ammonia treatment of nitroglycerin-containing propellants is complicated by an exothermic reaction between ammonia and nitroglycerin. If not removed, the heat generated by this reaction can cause propellant ignition. To help design safe treatment processes, a model for the ammonia-propellant reaction was developed, which integrates transient energy and species conservation equations to simulate ammonia diffusion, heat generation, and heat flow in a propellant and in the solid residue resulting from ammonia treatment. It was calibrated using residue thickness and thermocouple data for one propellant. The calibrated model was used to predict conditions leading to ignition of thin propellant strips. The results agree well with experimental observations.

Introduction

With the end of the Cold War, safe, environmentally sound separation, recycling, and disposal of ingredients in solid rocket propellants and munitions has become a national priority. Solid rocket propellants typically contain three main components: a fuel, usually powdered aluminum or other metals; oxidizers, usually particulate ammonium perchlorate (NH_4ClO_4 or AP), HMX (1,3,5,7-tetranitro-1,3,5,7-tetraazacyclooctane), or both; and a polymeric binder that holds the fuel and oxidizer particles together. One way to dispose of solid propellants is incineration. For AP-containing propellants, however, incineration produces a large amount of hydrogen chloride that must be scrubbed from the products before they are released to the environment.

An alternative to burning the whole propellant is to extract AP prior to incineration. A proposed separation technique (McBride and Thun, 1979; Matson et al., 1988; Melvin, 1989, 1992, and 1994a,b; Reader et al., 1993; Hendrickson et al., 1993; Losee et al., 1993; Stevens et al., 1994) uses liquid ammonia to extract both AP and HMX. The solid residue is depleted of HCl-producing AP and is less sensitive to impact and other forms of accidental initiation. In addition, fairly pure AP and HMX can be recovered from the extract and used in other applications.

Some propellants contain nitroglycerin (glycerol trinitrate or NG) as a binder ingredient. For these propellants, ammonia treatment is complicated by an exothermic reaction between NG and ammonia. If heat released by this reaction is not removed, the propellant can ignite.

Figure 1 summarizes the physical and chemical processes important in the reaction of ammonia with an NG-containing propellant. Ammonia diffuses into the solid, dissolves AP and HMX crystals and leaves solution-filled voids behind. NG in the binder is chemically destroyed, but the rest of the binder remains relatively intact. The dissolved oxidizers leach into the external fluid, leaving a solid residue or crust depleted of AP, HMX and NG. Ammonia must diffuse through the fluid entrained in this growing crust to react with fresh propellant.

Heat generated at the reaction zone is conducted into the fresh solid propellant and into the crust. For propellant immersed in liquid ammonia, reaction-generated heat is readily removed by boiling. When designing contingency plans for a treatment process, however, one cannot assume that the solid will always be immersed in liquid. Under some circumstances, propellant may be exposed to ammonia vapor. Heat removal is much less effective in vapor than in liquid and

Correspondence concerning this article should be addressed to R. L. Raun at his current address: 320 North Main, Lindon, UT 84042.

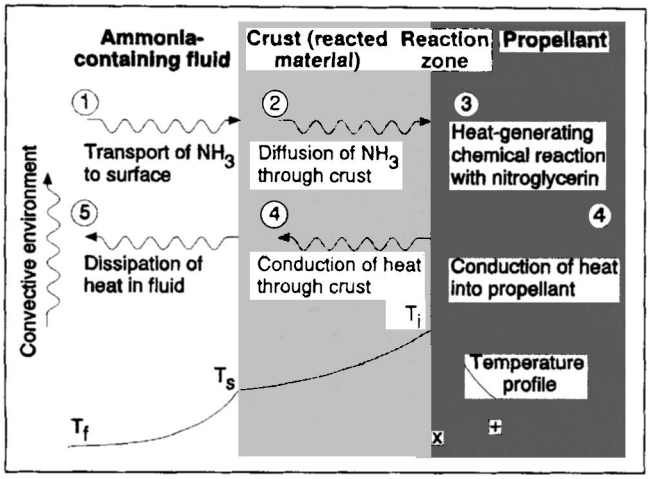

Figure 1. Processes simulated by the ammonia-propellant reaction model.

heat can build up, possibly leading to ignition of the solid propellant.

Heat management is clearly an important issue in designing safe, ammonia-based treatment processes for NG-containing propellants. Heat generation rates need to be assessed, especially for conditions where exposure to ammonia gas is possible. A computer-based model has been developed for this purpose. This model is applicable to the 1-D geometry and includes mathematical descriptions of the processes in Figure 1. It models progressive consumption of propellant and generation of a product layer (crust).

This article describes development and demonstration of this computer model. Theory is described in the Model Development section. The Model Calibration section describes calibration, wherein input parameters were adjusted to give the best fit between model predictions and a set of target data. This procedure gave a good fit between predictions and the target data. The target data were of two types. One type was temperature measured in experiments in which small, thermocouple-instrumented blocks of propellant were exposed to ammonia gas. The other data were measurements of the growth of the residue layer as a function of time. These experiments are described briefly in the Experimental section. Conditions leading to ignition of thin propellant strips were investigated experimentally and simulated successfully with the calibrated model. Results of the experiments, model calibration, and ignition studies are discussed in the Results section.

Model Development

The ammonia-propellant reaction model estimates transient temperature and concentration profiles in a slab of solid propellant and in a condensed phase product layer produced by reaction with ammonia. The model is general in that it allows for exposure of a propellant that contains any ammonia-soluble ingredient (not just AP) and any ammonia-reactive ingredient (not just NG) to a liquid or gas mixture that contains ammonia. In fact, the model can be used for propellants that contain more than one soluble or more than one reactive ingredient, although ingredients of each kind must be treated as one soluble and one reactive with "average" properties. Since the model is general, the development described below is general. However, conditions leading to ignition of an AP- and NG-containing propellant exposed to pure ammonia gas were of primary interest to us and these were the conditions modeled in all simulations described in this article.

The model was based on a shrinking core heterogeneous reaction model like that described by Levenspiel (1972). Figure 1 summarizes the main transport processes involved. One of three processes controls the reaction rate: transport of ammonia from the bulk fluid to the solid surface, diffusion of ammonia through the crust, and reaction with propellant ingredients at (or near) the fresh propellant surface. Three processes affect the temperature of the solid: heat generation from the reaction, conduction of heat through the crust and into the propellant, and dissipation of heat into the fluid environment. Mathematical descriptions of these processes follow, but first it is helpful to describe some additional characteristics of the ammonia-propellant reaction.

Characteristics of the ammonia-propellant reaction

Experiments in which blocks of an AP- and NG-containing propellant were exposed to saturated (295 K, 0.89 MPa) ammonia vapor revealed the following characteristics of the ammonia-propellant reaction. These characteristics were considered in developing the model:

- Liquid (mostly ammonia with dissolved AP) exudes from the surface during exposure. After exposure, more liquid is obtained by squeezing the spongy solid residue. From these observations, we conclude that liquid-filled voids (that is, the holes left by dissolved oxidizer particles) are formed, whether the propellant is exposed to liquid or gaseous ammonia.
- Cutting open a treated block reveals a surface layer discolored by the ammonia-NG reaction. To the naked eye, the boundary between discolored and fresh propellant is very sharp. This suggests that the reaction occurs in a thin zone. Using a magnifying glass, however, it is seen that AP crystals dissolve slightly before the binder becomes discolored. This suggests that the NG reaction lags slightly behind the dissolution process. Thus, for large propellant chunks (that is, large compared to the reaction zone thickness), it may be acceptable to treat dissolution of solubles and reaction of energetic species as if they occur in one infinitesimally thin zone. For thin propellant strips (thickness on the order of the reaction zone), however, it may be necessary to treat dissolution and reaction separately. The process was modeled both ways; the results are compared in the Results section.
- The mechanism and stoichiometry of the ammonia–NG reaction is not well-understood. Laboratory analysis of liquid exudate indicates that reaction products include ammonium salts (such as nitrate and nitrite) and partially denitrated derivatives of NG. Based on this observation, the reaction probably includes many elementary steps. We chose to model the reaction using overall chemistry rather than attempting a mechanistic approach.

Modeling of the ammonia-propellant reaction

The ammonia-propellant reaction was modeled using two generalized reaction schemes. The first is a one-step process

defining the overall reaction chemistry. The entire process, including dissolution of soluble components, chemical reaction of ammonia with energetic components, and the associated heat release, was assumed to occur in an infinitesimally thin zone.

The second process involves two steps. The first step is dissolution of soluble ingredients. As with the one-step process, this step occurs in a thin zone. This step was assumed to create liquid-filled voids and to release energetic components bound in the propellant.

The second step is a volumetric reaction that occurs distributed throughout the crust. This step was used to model the exothermic reaction between ammonia and the energetic components released by the first step. This choice of reaction sequence (dissolution followed by distributed reaction) implies that little reaction with the energetic components is likely until dissolution of soluble components enhances ammonia diffusion by creating liquid-filled voids.

Interfacial reaction

The one-step reaction (or first step of the two-step reaction) was described by

$$P + \mu_A A \rightarrow \mu_I I + \mu_R R \tag{1}$$

where P, A, and I represent propellant, ammonia, and inert products, and R represents reactive ingredients released from the propellant by this step; μ_A is the mass of ammonia used, and μ_I and μ_R are the masses of inerts and reactive species produced per unit mass of propellant.

An essential feature of this step is dissolution of soluble ingredients by ammonia. Although dissolution is *not* a chemical reaction, it was convenient to treat it as a reaction in the modeling. Dissolution is an equilibrium process, that is, it will not occur if the liquid is saturated with solute. To take equilibrium into account, the rate equation for Eq. 1 was written as

$$-r''_{Ai*} = k_i \rho_c (w_{Ai} - w_{A,\mathrm{eq}}) \tag{2}$$

where $-r''_{Ai*}$ is the ammonia "usage" rate (kg/m^2·s), w_{Ai} is the ammonia mass fraction at the interface (based on all materials in the crust, not just entrained liquid), ρ_c is the average product density (including entrained liquid, kg/m^3), k_i is a rate constant (m/s), and $w_{A,\mathrm{eq}}$ is the ammonia mass fraction at saturation (again, based on all materials). Thus, the rate was assumed to be proportional to the difference between the ammonia concentration and that which would prevail at saturation. If the process is rapid ($k_i \rightarrow \infty$), Eq. 2 reduces to $w_{Ai} = w_{A,\mathrm{eq}}$.

For the one-step process, soluble propellant ingredients are dissolved and energetic components are destroyed in this step. Since no energetic components escape the reaction zone, $\mu_R = 0$ in Eq. 1. Both μ_A in Eq. 1 and the ammonia "usage" rate $-r''_{Ai*}$ in Eq. 2 include the amount of ammonia required to dissolve solutes and to destroy reactive ingredients in the propellant.

Heat generation associated with the interfacial reaction was modeled by

$$\lambda_c \left.\frac{\partial T}{\partial x}\right|_{i^-} = \lambda_p \left.\frac{\partial T}{\partial x}\right|_{i^+} + \rho_p u_i \Delta H_i \tag{3}$$

where subscripts i^- and i^+ denote conditions on the crust and unreacted sides of the interface, T is temperature (K), λ_c and λ_p are thermal conductivities (W/m·K) of the crust and propellant, and ΔH_i is the heat of reaction (which includes heat of solution for soluble materials in J/kg propellant); u_i is the reaction "velocity," that is, the rate at which the interface between the propellant and crust moves into the unreacted solid. From the stoichiometry in Eq. 1, this velocity is given by

$$u_i = -\frac{r''_{Ai*}}{\mu_A \rho_p}. \tag{4}$$

If the reaction is rapid ($k_i \rightarrow \infty$), then the rate is diffusion-limited. In this case, u_i is fixed by the rate at which ammonia diffuses to the reaction zone and is given by

$$u_i = -\frac{\rho_c}{\mu_A \rho_p} D_A \left.\frac{\partial w_A}{\partial x}\right|_i \tag{5}$$

where D_A is the effective diffusivity of ammonia in the crust (m^2/s).

The distributed reaction

In the two-step process, energetic components released by the first step react with ammonia in the second. Thus, $\mu_R \neq 0$, μ_A and $-r''_{Ai*}$ only include ammonia required for dissolution and ΔH_i only includes heat of solution. The distributed reaction was assumed to be of the form:

$$R + aA \rightarrow \text{Products} \tag{6}$$

where a is the mass of ammonia consumed per unit mass of R. This reaction was assumed to follow a second-order, irreversible rate equation:

$$-r'''_{Ad} = k_d \rho_c^2 w_A w_R \tag{7}$$

where $-r'''_{Ad}$ is the volumetric rate of disappearance of ammonia, w_R is the mass fraction of reactive ingredients, and k_d is a rate constant. The heat release rate per unit volume (W/m^3) from this reaction was given by $\dot{Q} = r'''_{Ad} \Delta H_d / a$ where ΔH_d is the heat of reaction per unit mass of R.

Mass (ammonia) and thermal diffusion

Ammonia diffusion and heat flow in the crust and propellant were modeled by the species and energy conservation equations. For one-dimensional, rectilinear flow, these equations are

$$\frac{\partial}{\partial t}(\rho w_j) + \frac{\partial}{\partial x}(\rho u w_j) = \frac{\partial}{\partial x}\left(\rho D_j \frac{\partial w_j}{\partial x}\right) + r'''_j \tag{8}$$

$$\frac{\partial}{\partial t}(\rho C T) + \frac{\partial}{\partial x}(\rho u C T) = \frac{\partial}{\partial x}\left(\lambda \frac{\partial T}{\partial x}\right) + \dot{Q} \tag{9}$$

where u is velocity (m/s), D_j is the effective diffusivity of species j (m^2/sec), r_j''' is the volumetric generation rate of species j (kg/m^3·s), C is heat capacity (J/kg·K), and $\dot{Q}$ is the volumetric heat generation rate (W/m^3). In the absence of distributed reactions, r_j''' and $\dot{Q}$ are zero. For both the one- and two-step reaction sequences, one species continuity equation was required for ammonia. For the two-step option, another was required for the reactive ingredients (R).

Boundary and interface continuity conditions

To obtain a complete solution from the conservation equations, boundary conditions at the fluid-crust boundary and continuity conditions at the crust-propellant interface were required.

At the fluid-crust boundary, a convective boundary condition was applied. For heat transfer, this condition was given by

$$q_s = -\lambda_c \left.\frac{\partial T}{\partial x}\right|_s = h(T_f - T_s) \tag{10}$$

where q_s is the heat flux into the surface per unit area (W/m^2), h is the fluid phase heat-transfer coefficient (W/m^2·K), and T_s and T_f are the surface and bulk fluid temperatures (K), respectively.

The convective condition for mass transfer was analogous to Eq. 10:

$$J_{As} = -\rho_c D_A \left(\frac{\partial w_A^{(i)}}{\partial x}\right)_s = h_m\left(w_{Af}^{(e)} - w_{As}^{(e)}\right) \tag{11}$$

where J_{As} is the flux of ammonia into the surface per unit area (kg/m^2·s), h_m is the mass-transfer coefficient (kg/m^2·s), and $w_{As}^{(e)}$ and $w_{Af}^{(e)}$ are the surface and bulk fluid ammonia mass fractions, respectively. The superscripts (i) and (e) indicate mass fractions in the crust (as based on all materials) and in the external fluid (unless otherwise specified, w_A with no superscript refers to crust weight fraction). To relate the external to the internal (crust) mass fraction at the surface, another equation was required. In the model, the following was used:

$$w_{As}^{(i)} = K w_{As}^{(e)}. \tag{12}$$

Basically, this is an equilibrium equation, that is, it relates the ammonia mass fractions that exist in equilibrium in the crust and external fluid. K may be affected by pressure, temperature, and composition, but we treated it as a constant. Assuming that pure ammonia is the external fluid, K was estimated from $K = \rho_c/(\rho_{Al}\epsilon)$ where ρ_{Al} is the density of liquid ammonia and ϵ is the porosity of the crust; ϵ was assumed to be the volume fraction of soluble ingredients in the propellant.

One of two boundary types was applied at the extreme righthand interface (as shown in Figure 1): symmetric (a two-sided mass of propellant or with an insulated right face) or convective. For the convective condition, the right propellant surface was assumed to be chemically inert but not thermally insulated. This allowed the model to simulate experiments in which one side of a propellant block was coated with a thin layer of silicone rubber sealer to prevent reaction. A separate heat-transfer coefficient was allowed for heat loss from this surface, but the same fluid temperature was used as for the reactive face.

At the crust–propellant interface, two conditions were imposed to link the crust and propellant energy equations. These required continuity of heat flux (Eq. 3) and temperature: $T_{i-} = T_{i+}$. For mass conservation, the condition $\rho_p u_i = \rho_c u_c$ was imposed, where u_c is the velocity at which the crust "moves away" from the interface. This condition requires that the mass flux of crust away from the interface is equal to the mass flux of propellant into the interface. If the crust has the same density as the propellant, then $u_c = u_i$; otherwise, the propellant block swells ($u_c > u_i$) or shrinks ($u_c < u_i$) as the reaction progresses.

Continuity in species mass flux was required by satisfying the following equation:

$$-J_{ji} = \rho_c\left(u_c w_j + D_j \frac{\partial w_j}{\partial x}\right)\bigg|_i = r_{ji}'' \tag{13}$$

where J_{ji} is the mass flux of species j per unit area (kg/m^2·s) into the interface, and r_{ji}'' is the rate of production of j at the interface. For the reactive ingredients (released according to Eq. 1), $r_{Ri}'' = \mu_R \rho_p u_i$. For the one-step option, μ_R is 0; for the two-step option, μ_R is the mass fraction of the reactive ingredients in the fresh propellant.

For ammonia, r_{Ai}'' ($= -J_{Ai}$) in Eq. 13 differs from r_{Ai*}'' in Eq. 2. r_{Ai}'' is given by:

$$-r_{Ai}'' = \mu_{AR}\rho_p u_i \tag{14}$$

where μ_{AR} is the mass of ammonia chemically destroyed at the interface (by the first reaction step) per unit mass of propellant: $-r_{Ai}''$ is the rate at which ammonia is destroyed; $-r_{Ai*}''$ includes this rate plus the rate at which ammonia must be supplied to the interface to dissolve solutes. For the two-step option, no ammonia is chemically destroyed at the interface, thus, $\mu_{AR} \equiv 0$ and $r_{Ai}'' \equiv 0$.

Numerical solution of the conservation equations

The method used to solve conservation Eqs. 8 and 9 was based on Patankar's (1980) method for solving combined convection and diffusion problems. Application of this method to these equations gave tridiagonal systems of algebraic equations. These systems were solved iteratively by the method of successive substitution to obtain temperatures and ammonia and reactive component weight fractions at discrete time steps.

As the reaction proceeds, propellant is consumed and crust is formed. Thus, the fresh propellant shrinks while the crust grows. In the numerical solution, this phenomenon was modeled by adding crust elements and by subtracting propellant elements as time progressed.

Model Calibration

Physical and chemical properties required as input to the ammonia-propellant reaction model were identified and esti-

Table 1. Summary of Initial Property Estimates Used in Ammonia-Propellant Model

Description	Value
Propellant dens., ρ_p	1,853 kg/m^3
Propellant thermal cond., λ_p	0.36 W/m·K
Propellant heat capacity, C_p	1,214 J/kg·K
Crust density, ρ_c	1,853 kg/m^3
Crust thermal cond., λ_c	0.36 W/m·K
Crust heat capacity, C_c	1,214 J/kg·K
Effective diffusivity, D_A	5.06×10^{-9} m^2/s
Equilibrium constant, K	0.112
Heat-transfer coeff., h	41.6 W/m^2·K
Interf. reaction rate const., k_i	1.82×10^{-5} m/s
One-Step Reaction Option ($k_d = 0$)	
Ammonia/propellant mass ratio, μ_A	0.0773 kg A/kg P
Heat of reaction, ΔH_i	7.04×10^5 J/kg P
Two-Step Reaction Option ($k_d > 0$)	
Ammonia/propellant mass ratio, μ_A	0.0644 kg A/kg P
Heat of reaction, ΔH_i	0 J/kg P
Equilib. ammonia mass fraction, $w_{A,eq}$	0.0644 kg A/kg crust
Distributed reaction rate constant, k_d	0* s^{-1}
Distributed reaction heat of reaction, ΔH_d	$4.09\times10^{6\dagger}$ J/kg R
Ammonia/reactive mass ratio, a	0.075 kg A/kg R
Mass fraction reactive in propellant, μ_R	0.1722 kg R/kg P

*Initial value only; adjustment during calibration gave $k_d > 0$ (Table 3).
†ΔH_d set to $\Delta H_{i,\text{one-step}}/\mu_R = 7.04\times10^5/0.1722 = 4.09\times10^6$ to ensure that the same amount of heat was generated per unit mass of propellant for both options.

mated. Some inputs, such as propellant thermal properties were obtained from the Hercules propellant database (Hercules, Inc., 1987). Other parameters were estimated from quasi-steady analysis of experimental data using simplified, steady-state versions of Eqs. 8 and 9. The heat of reaction for the ammonia-propellant reaction was estimated from differential scanning calorimetry (DSC) results for a solid propellant in 0.4 MPa ammonia gas. From these estimates, program input was prepared for a propellant containing approximately 17% NG by weight. The input is summarized in Table 1.

To obtain the best correspondence between experimental data and model predictions, adjustment of some input parameters (that is, calibration) was required. An unconstrained optimization program was used to obtain the best "least-squares" fit between model predictions and a set of target data. The target data were crust thickness measurements and transient temperatures from thermocouple instrumented block tests. These tests are discussed below.

In its calibration mode, the model requires time-varying fluid temperature as input. A cubic spline smoothing algorithm was used to remove noise from fluid temperature data. Figure 4 shows a comparison of the smoothed data to average thermocouple data from six block tests.

Model Application

The calibrated input was used to simulate ignition experiments in which 2, 3 and 4 thin (0.9 mm) strips of propellant were exposed to ammonia gas at 0.89 MPa in a closed vessel. This required coupling of the ammonia-propellant reaction model to a well-stirred batch reactor model. The batch reactor model simulated the effect of heat generation from a specified volume of propellant particles on the fluid temperature in the vessel.

The fluid temperature in the vessel was modeled by the differential equation

$$m_f C_f \frac{dT_f}{dt} = h a_p V_p (T_s - T_f) - U_e A_e (T_f - T_e) \qquad (15)$$

where m_f and C_f are the mass (kg) and heat capacity (J/kg·K) of the fluid. In posing Eq. 15, we assumed that particles are of uniform size and surface temperature and that fluid temperature is uniform throughout the vessel. The first term on the righthand side of Eq. 15 gives the rate of heat transfer from the particles to the fluid, where h is the coefficient for convective heat transfer between the particles and fluid (same as h in Eq. 10), a_p is the particle surface area per unit volume (m^{-1}), V_p is the particle volume (m^3), and T_s is the particle surface temperature (K).

The second term models heat loss to the surroundings through an overall heat-transfer coefficient, U_e (W/m^2·K); A_e is the vessel wall area available for heat transfer (m^2), and T_e is the temperature of the surroundings. U_e was estimated from an empirical correlation for natural convection heat transfer (Bird et al., 1960). This estimate was adjusted to match the predicted maximum gas temperature with the average of maxima observed in two-strip tests.

Experimental

To obtain data for model calibration and application, solid propellant samples were exposed to 295 K gaseous ammonia at 0.89 MPa. Three types of tests were conducted. These tests are described below. All tests were conducted inside small pressure vessels.

Instrumented block tests

To provide data required for model calibration, tests were performed with thermocouple-instrumented $25\times25\times12$ mm blocks of propellant. The experimental setup is shown in Figure 2. Two thermocouples were embedded in the block approximately 1/4 and 1/2 of the way from one 25×25 mm surface. The rear face and edges were potted with silicone rubber sealer to prevent reaction and intrusion of ammonia along the thermocouple leads.

The instrumented block was placed in an aluminum foil pan inside of a pressure vessel. Another thermocouple was pressed gently against the surface. A fourth thermocouple was used to measure the gas temperature.

The vessel was sealed and pressurized with gaseous ammonia. Thermocouple temperatures were recorded as a function of time by a PC-based data-acquisition system.

Crust thickness measurements

To obtain crust thickness measurements required for model calibration, blocks of propellant were placed in a vessel and exposed to gaseous ammonia for 1, 2, 5, 10, 15, 20 and 40 min. Following exposure, the blocks were removed and cut open to reveal the interior. The ammonia-exposed surface layer showed discoloration due to the reaction between ammonia and NG. Under a magnifying glass, the thickness of the discolored layer was measured with a scale.

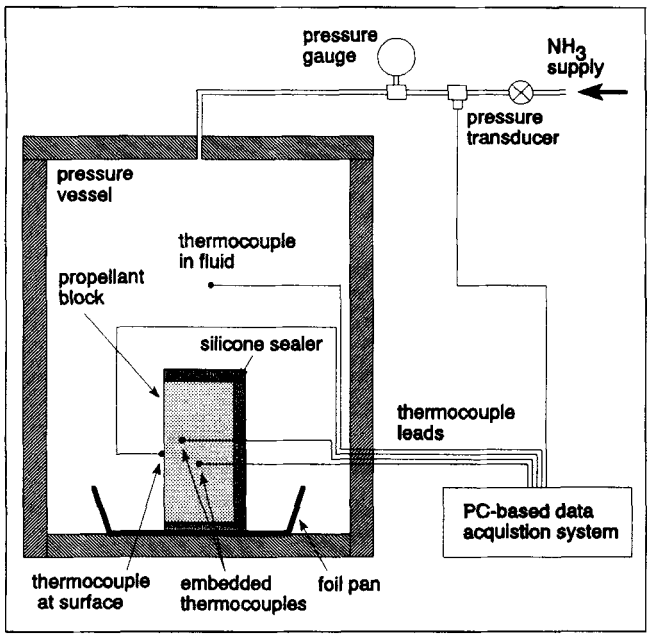

Figure 2. Experimental apparatus used in thermocouple instrumented block tests.

Strip ignition tests

An essential consideration in designing a safe ammonia treatment process is determining the rate of heat removal required to keep the temperature below the propellant ignition point. As shown in Eq. 15, the rate of temperature rise in the fluid (dT_f/dt) is proportional to the rate of heat generation minus the rate of heat loss to the environment. The rate of generation is proportional to the reactive surface area of the propellant; the rate of heat loss to the environment is proportional to the vessel surface area. In light of these considerations, experiments were done to determine the propellant surface area at which natural convection heat loss from a small vessel became inadequate to prevent ignition. For the same propellant formulation used in the block tests, two, three and four 0.9-mm-thick strips of propellant were suspended in a small plexiglass enclosure within a pressure vessel as shown in Figure 3. Thermocouples were placed in the gas both inside and outside of the enclosure. The vessel was sealed and pressurized with gaseous ammonia. Temperature was recorded as a function of time and the strips were watched for ignition.

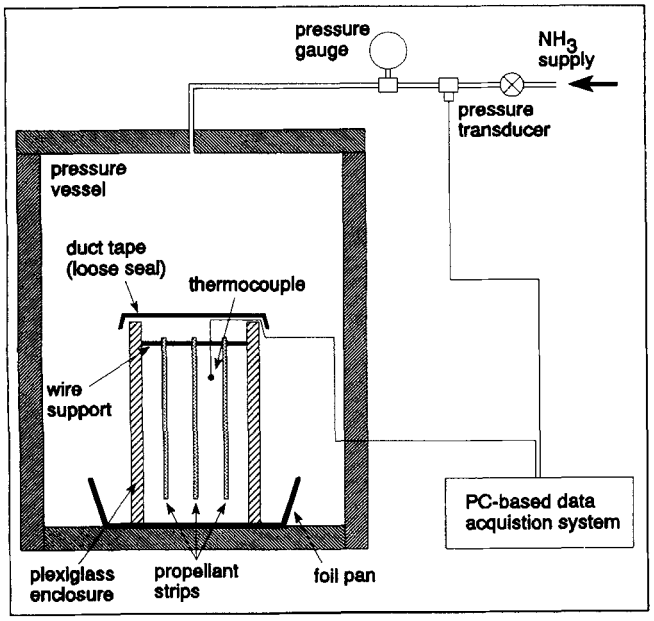

Figure 3. Experimental apparatus used in strip ignition tests.

Results

Instrumented block tests

Six thermocouple instrumented block tests were performed with the 17% NG propellant. Since differences in measured temperatures among the tests were significant (a standard deviation of 3.3 K), the thermocouples measurements for all six tests were averaged to make the plot shown in Figure 4. (Sources of variation include differences in block size, composition and placement in the vessel, and variation in thermocouple response and placement within the block.)

Immediately following exposure to ammonia, the propellant surface temperature began to rise, a manifestation of reaction-generated heat. Soon after, the embedded thermocouple temperatures began to rise, indicating conduction of heat into the interior of the block.

After approximately 10 min, the surface temperature reached a maximum and began to decrease, indicating movement of the reaction zone deeper into the block. The embedded thermocouple temperatures rose for about 10 more min; then they became approximately constant. This indicated that the block had attained a "quasi-steady" condition where the rate of heat loss to the gas was approximately equal to the rate of heat generation.

Diffusion tests

Figure 5 shows crust thickness plotted against square root of time. There is scatter; however, the data approximately follow a linear trend.

One of three processes (Figure 1) controls the effective reaction rate: transport of ammonia from the bulk fluid to the outer (crust) surface, ammonia diffusion through the crust to the fresh propellant surface, or chemical reaction at that surface. As shown by Levenspiel (1982), if fluid phase transport or chemical reaction controls, the effective reaction rate is approximately constant in time. Thus, the crust thickness increases linearly with time. If crust diffusion controls, the effective rate is inversely proportional to the crust thickness. Thus, the effective rate decreases with time and the crust thickness increases linearly with the square root of time.

In reality, more than one mechanism controls over a long time. Initially there is no crust and thus no resistance due to crust diffusion. Thus, either the kinetic or fluid mass-transfer process controls at first. As the crust grows, the crust resistance increases until it becomes controlling. Thus, crust thickness should begin by varying linearly with t and then shift to linear variation with $t^{1/2}$. The data in Figure 5 appear to show this behavior.

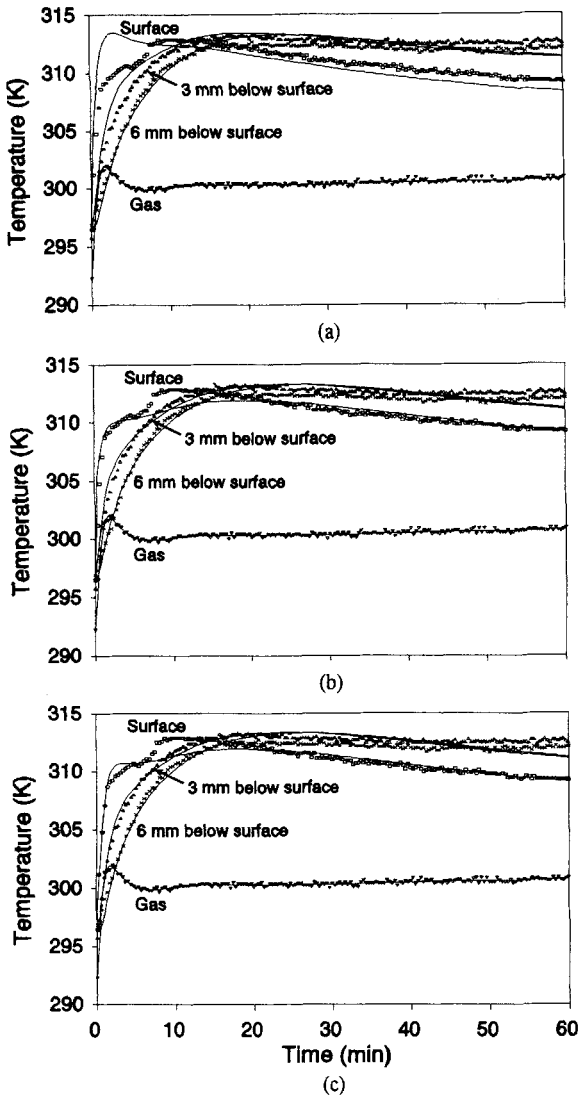

Figure 4. Average temperature data from six thermocouple-instrumented block tests.

Solid lines show temperatures predicted by model using calibrated input sets (a) A; (b) B; and (c) C.

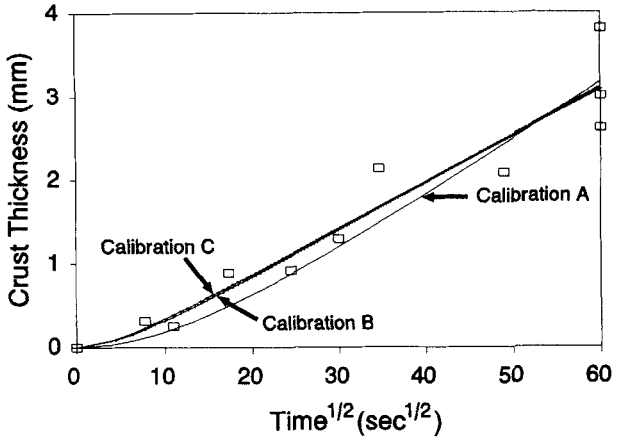

Figure 5. Crust thickness measurements.

Lines show thicknesses predicted by model using calibrated input sets A, B, and C.

Strip ignition tests

Maximum temperatures and times to reach maximum temperature for the strip tests are listed in Table 2. As can be seen, the maximum temperature increased from two to three strips. For four strips, however, the temperature did not reach a maximum. Instead, the strips ignited and burned at the times and temperatures indicated.

Instrumented block simulations

In addition to data, Figures 4 and 5 show the results of model predictions of temperatures and crust thickness. These predictions were for sets of adjusted input parameters that gave the best "least-squares" fit to the data. Table 3 summarizes three sets of parameters. Calibrations A and B used the one-step reaction option; calibration C used the two-step option. In B and C, propellant thermal conductivity and heat of reaction were adjusted; in A, they were not. The adjusted heat of reaction was lower than the DSC-derived estimate, suggesting that the reaction in the block test did not reach the degree of completion observed in DSC tests.

Figure 4a shows results for calibration A. The predictions matched the data trends fairly well; however, the predicted difference between the embedded thermocouple temperatures was larger than the observed difference at short times ($t < 10$ min). Figure 4b shows results when propellant thermal conductivity and heat of reaction were adjusted (calibration B). The agreement between the experiment and simulation was much improved.

Table 2. Pressure Vessel Tests with $50 \times 25 \times 0.9$ mm Propellant Strips Inside a Plexiglass Tube

Test No.	No. of Strips	Time to Max. Temp. (min)	Max. Temp. (K)	Ignition (Y/N)?
1	2	15	342	N
2	2	10	362	N
3	3	13	385	N
4	3	7	395	N
5	4	7	364	Y
6	4	7	374	Y

Table 3. Input Parameters Giving Best Least-Squares Fit of Block Test Thermocouple and Crust Thickness Data

Parameter*	Calibration A	Calibration B	Calibration C
λ_p	(0.36)†	0.541	0.530
λ_c	0.845	0.477	0.439
D_A	4.32×10^{-9}	4.58×10^{-9}	4.59×10^{-9}
K	0.126	0.0962	0.0943
h	102	35.5	35.5
k_i	2.60×10^{-6}	1.22×10^{-5}	1.24×10^{-5}
ΔH_i	(7.04×10^5)	3.01×10^5	(0)
k_d	—	—	0.469
ΔH_d	—	—	1.76×10^6
U_e ‡	12.1	6.69	6.81

*See Table 1 for definitions and units.
†Parameters in parentheses were not adjusted during calibration.
‡Not calibrated using block test data; only used in strip ignition simulations; units: W/m^2·K.

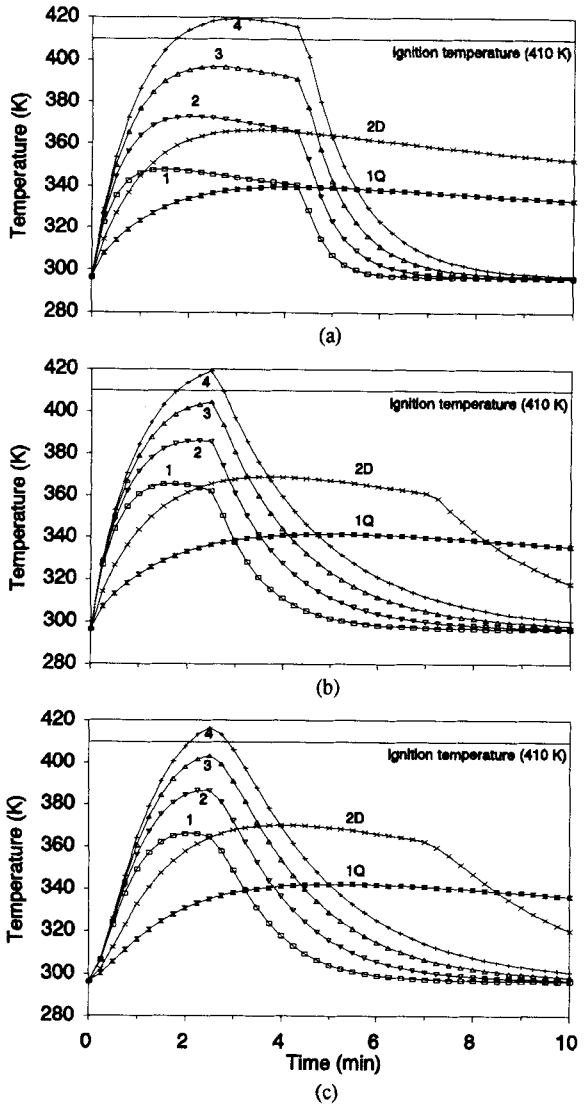

Figure 6. Temperatures of 50 mm × 25 mm strips of propellant in a 90-mL ammonia-filled vessel, predicted by model using calibrated input sets: (a) A; (b) B; and (c) C.

Curves 1–4 are for the corresponding number of 0.9-mm-thick strips; 2D is for two 1.8-mm-thick strips; 1Q is for one 3.6-mm-thick strip.

Figure 4c shows results for calibration C. Compared to B, the improvement in fit was slight and occurred mainly at short times. Thus, addition of distributed reaction was not very important for modeling the behavior of propellant blocks of the size used in these tests.

Figure 5 shows that crust thickness predictions for B and C (in which heat of reaction was adjusted) fit the data well; those for A gave a poorer fit. Thus, crust thickness was fit well only when using a lower heat of reaction than estimated from DSC data.

Strip ignition simulations

The calibrated model was used to simulate strip ignition tests. To assess the effect of the one- and two-step reaction options and variation in other model parameters, all calibrations in Table 3 were used. For each, the overall heat-transfer coefficient for heat loss to the environment (U_e) was adjusted to make the predicted maximum gas temperature for a two-strip test equal to 352 K, the average of the observed maxima (listed in Table 2).

Figure 6a shows model predictions of propellant temperature for one, two, three and four strips of propellant using the input parameters from calibration A. As can be seen, the model predicted increasing maximum temperature for successive numbers of strips. From thermal ignition data (Butcher, 1991), the propellant was known to have an ignition temperature of approximately 410 K. Figure 6a shows that for three strips, the maximum temperature predicted was 398 K. Thus, the model predicted that three strips should not ignite. For four strips, however, the maximum temperature was 420 K. Thus, the model predicted that four strips should ignite. These results agree with the experimental results.

Figures 6b and 6c shows results for the same simulation, but using input parameters from calibrations B and C. For both calibrations, the predicted temperature maxima for three and four strips are below and above the ignition temperature, respectively. Thus, these model predictions led to the same conclusion as for calibration A.

As described in the previous section, adding distributed reaction (that is, using the two-step option) made little difference in the model's ability to fit temperature and crust thickness data for blocks. Figures 6b and 6c show that distributed reaction also had little effect on the shapes of the temperature–time profiles for thin strips. Thus, including distributed reaction was not important for either blocks or thin strips of this propellant. However, the shape of the profile for calibration A (Figure 6a) differs dramatically from that for B. The heat of reaction used in B was much lower than for A. Thus, although accurate heat of reaction may not be critical for modeling large blocks (both A and B did a fair job of matching the block temperature data shown in Figure 4), it appears to be important for modeling thin strips (and by inference, small particles).

Figure 7 compares predicted maximum gas temperatures to experimental maximum thermocouple temperatures in the

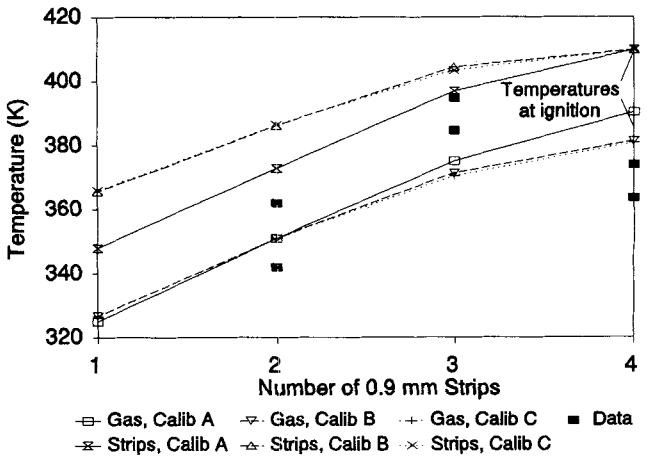

Figure 7. Maximum gas and strip temperatures predicted by model compared to maximum temperature data from strip ignition tests.

strip tests. There is lack of agreement for three and four strips. Possible explanations for these discrepancies are:

(1) Experimental error exists: the discrepancies are within the range of data variation.

(2) During most tests, the propellant strips were observed to curl. This usually caused contact between the strips. This may have caused the thermocouple to contact the propellant. In these cases, the thermocouple measured propellant, not gas temperature.

(3) Another effect of strip contact is reduction in reactive surface area. This reduces heat generation rate and maximum temperature. That predicted strip and gas temperatures for three strips bracket the experimental results is consistent with this and explanation 2.

(4) The model ignores the temperature dependency of condensed phase diffusivity. Including this effect could alter the temperature–time profile and the positions and magnitudes of temperature maxima. Temperature-dependent diffusivity could also explain why predicted temperature maxima occurred earlier (on the order of 2–4 min) than the observed maxima (7–15 min).

Conclusions

A computer model for simulating heat release from the reaction of ammonia and nitroglycerin-containing solid rocket propellants has been developed. An unconstrained optimization program was used to adjust (calibrate) input parameters to give the best fit between predictions and a set of target data. The target data were of two types: crust thickness measurements and temperatures from tests in which blocks of propellant instrumented with thermocouples were exposed to gaseous ammonia. Good fits between predictions and experimental results were achieved for a propellant using two reaction models and three sets of input parameters.

After calibrating the model, it was used to predict conditions leading to ignition of thin propellant strips. For all three sets of calibrated input parameters, the model predicted ignition under the same conditions as observed experimentally. However, the shape of the predicted temperature–time profiles for the thin strips varied significantly among the three calibrations. The factor that affected profile shape the most was heat of reaction. Thus, accurate heat of reaction is important to accurate modeling of the behavior of thin strips (or small particles).

Acknowledgments

The authors wish to thank Mr. Wilford Phillips of Hercules Bacchus Works who performed the experiments and Dr. George Dugan at the Hercules Research Center who performed DSC testing in pressurized ammonia gas to provide heat of reaction estimates.

Literature Cited

Bird, R. B., W. E. Stewart, and E. N. Lightfoot, *Transport Phenomena*, Wiley, New York, p. 646 (1960).

Butcher, A. G., "Propellant Response to Cook-off as Influenced by Binder Type: II. Effects of Confinement," *Joint AIAA/ASME/SAE/ASEE Propulsion Conf.*, AIAA, New York (1991).

CPIA Publications, Chemical Propulsion Information Agency, Johns Hopkins Univ., Columbia, MD.

Hendrickson, K. A., L. A. Losee, P. M. Stevens, and D. M. Mitchell, "Materials Hazards Testing in Support of the Army Large Rocket Motor Demilitarization Pilot Plant," *JANNAF Propulsion Meeting*, CPIA Pub. No. 602, Vol. 1, p. 79 (1993).

Hercules Incorporated Material Data File (electronic), Hercules Inc., Magna, UT, p. 203 (Aug. 14, 1987).

Levenspiel, O., *Chemical Reaction Engineering*, Chap. 12, Wiley, New York (1972).

Losee, L. A., L. J. Lyon, C. A. Ford, B. A. Hill, K. A. Hendrickson, P. M. Stevens, D. H. Mitchell, N. W. Rizzardi, W. S. Melvin, and P. G. Schirk, "Preliminary Hazards Testing and Analysis of the Liquid Ammonia Demilitarization Process," *JANNAF Propulsion Systems Hazards Meeting*, CPIA Pub. No. 599, Vol. 1, p. 225 (1993).

Matson, D. W., B. W. Wright, R. D. Smith, W. S. Melvin, and J. F. Graham, "Applications of Supercritical Fluid Systems to Solid Rocket Propellants," *JANNAF Propulsion Meeting*, CPIA Pub. No. 480, Vol. 3, p. 401 (1988).

McBride, W. R., and W. E. Thun, "Sensitivity and Characterization of Selected Liquid Ammonia Systems: Reclamation Methodology for Ammonium Perchlorate Propellants," Report No. NWC TP 6056, Naval Weapons Center, China Lake, CA (Apr., 1979).

Melvin, W. S., "Demilitarization Method for Composite Propellants," *JANNAF Propulsion Meeting*, CPIA Pub. No. 515, Vol. 3, p. 103 (1989).

Melvin, W. S., "Critical Fluid Demilitarization and Ingredient Reclamation Technology," Critical Technol. Rep., Propulsion Directorate, U.S. Army MICOM, Redstone Arsenal, AL (July, 1992).

Melvin, W. S., *Method to Extract and Recover Nitramine Oxidizers from Solid Propellants Using Liquid Ammonia*, U.S. Patent 5,284,995 (1994a).

Melvin, W. S., and J. S. Wright, "Recovery and Reuse of Rocket Motor Propellant Ingredients," *JANNAF Safety and Environmental Protection Meeting*, CPIA Pub. No. 614, Vol. 1, p. 427 (1994b).

Patankar, S. V., *Numerical Heat Transfer and Fluid Flow*, Chap. 5, McGraw-Hill, New York (1980).

Reader, G. E., D. H. Mitchell, K. K. Light, M. E. Morgan, P. G. Schirk, O. J. Manar, W. S. Melvin, and N. W. Rizzardi, "Process Development for Rocket Motor Demilitarization and Ingredient Recovery Using Ammonia," *JANNAF Safety and Environmental Protection Meeting*, CPIA Pub. No. 600, Vol. 1, p. 381 (1993).

Stevens, P. M., M. H. Reed, L. A. Losee, K. A. Hendrickson, and D. H. Mitchell, "Hazards Analysis of an Integral Class 1.1/1.3 Rocket Motor Demilitarization and Ingredient Recovery System Using Ammonia," *JANNAF Safety and Environmental Protection Meeting*, CPIA Pub. No. 614, Vol. 1, p. 227 (1994).

Manuscript received Feb. 22, 1994, and revision received Aug. 31, 1994.